Mutat Res Gen Tox En xxx (xxxx) xxx–xxx

Contents lists available at ScienceDirect

Mutat Res Gen Tox En

journal homepage: www.elsevier.com/locate/gentox

The comet assay applied to HepG2 liver spheroids

Elisabeth Elje[a], Michelle Hesler[b], Elise Rundén-Pran[a], Pascal Mann[b], Espen Mariussen[a], Sylvia Wagner[b], Maria Dusinska[a], Yvonne Kohl[b,*]

[a] NILU – Norwegian Institute for Air Research, Department for Environmental Chemistry, Health Effects Laboratory, Instituttveien 18, 2007 Kjeller, Norway
[b] Fraunhofer Institute for Biomedical Engineering IBMT, Department Bioprocessing & Bioanalytics, Joseph-von-Fraunhofer-Weg 1, 66280 Sulzbach, Germany

ARTICLE INFO

Keywords:
Liver spheroids
Advanced *in vitro* model
Genotoxicity
Comet assay
2D and 3D culture

ABSTRACT

In accordance with the 3 Rs to reduce *in vivo* testing, more advanced *in vitro* models, moving from 2D monolayer to 3D cultures, should be developed for prediction of human toxicity of industrial chemicals and environmental pollutants. In this study we compared cytotoxic and genotoxic responses induced by chemicals in 2D and 3D spheroidal cultures of the human liver cancer cell line HepG2.

HepG2 spheroids were prepared by hanging drop technology. Both 3D spheroids and 2D monolayer cultures were exposed to different chemicals (colchicine, chlorpromazine hydrochloride or methyl methanesulfonate) for geno- and cytotoxicity studies. Cytotoxicity was investigated by alamarBlue assay, flow cytometry and confocal imaging. DNA damage was investigated by the comet assay with and without Fpg enzyme for detection of DNA strand breaks and oxidized or alkylated base lesions.

The results from the cyto- and genotoxicity tests showed differences in sensitivity comparing the 2D and 3D HepG2 models. This study shows that human 3D spheroidal hepatocellular cultures can be successfully applied for genotoxicity testing by the comet assay and represent a promising advanced *in vitro* model for toxicity testing.

1. Introduction

In experimental toxicology, there is an ongoing shift towards increased use of *in vitro* models in compliance with the 3 Rs to reduce, replace and refine animal experiments. The importance of developing new advanced *in vitro* models, that decrease the costs and time for hazard characterization and risk assessment but still provide reliable results, is stressed in the Regulation made by the EU Registration, Evaluation, Authorization and restriction of Chemicals (REACH) (EC No 1907/2006) [1]. Also, *in vitro* models allow utilization of human cells, which might better reflect human effects than *in vivo* rodent models [2–4]. For standard *in vitro* models, the cells are grown in two dimensions. Compared to the *in vivo* situation, these models comprise limited intercellular signaling, which is an important aspect in cellular responses and cell survival after exposure to chemical compounds [3,4]. Thus, *in vitro* models with cells arranged in a three-dimensional (3D) structure, resembling cell organization of tissues and organs, are likely to better mimic responses in humans. The development of advanced 3D models has gained increased attention within the last two decades [5,6]. Models for the assessment of toxicity must reflect the *in vivo* situation as closely as possible. The existing 3D cell models vary widely due to the diverse requirements of different cell lines and applications, and each model has its own advantages and limitations [7–9].

Liver models are important for toxicity testing, as the liver is a main target organ for substances reaching systemic circulation and plays a central role in metabolism as well as the toxification and de-toxification of substances. Liver 3D models can be prepared by hydrogel, scaffold based technologies or spheroidal culture techniques [4,6,9]. Hepatocytes growing in spheroids have become a highly used 3D model, where monodispersed cells self-organize themselves into a spherical conformation as the adhesion to the culture substrate is prevented [4]. Cultures of primary human hepatocytes are considered as the gold standard for studying metabolism and toxicity [4,9,10]. However, because of difficulties associated with isolating and culturing of cells, costs and inter-donor variation, much research has been directed towards using alternatives, such as hepatic-derived cell lines [4,11].

The human hepatocellular carcinoma cell line HepG2 is frequently used in early safety assessment because of availability, unlimited cell

Abbreviations: 2D, two-dimensional; 3D, three-dimensional; ALT, alanine transaminase; AST, aspartate aminotransferase; CHLO, chlorpromazine hydrochloride; COL, colchicine; FDA, fluorescein diacetate; FPG, formamidopyrimidine DNA glycosylase; ECM, extracellular matrix; GDH, glutamate dehydrogenase; MMS, methyl methanesulfonate; PBS, phosphate buffered saline; PI, propidium iodide; SEM, standard error of the mean; SBs, strand breaks

* Corresponding author.
E-mail address: yvonne.kohl@ibmt.fraunhofer.de (Y. Kohl).

https://doi.org/10.1016/j.mrgentox.2019.03.006
Received 21 November 2018; Received in revised form 6 March 2019; Accepted 15 March 2019

growth and high reproducibility of results [12,13]. The HepG2 cell line has many liver-specific functions [14–16] and is used as a screening model for cytotoxic substances and to study the metabolism of xenobiotics [17]. The cells are highly differentiated and reflect the liver activity of human parenchymal liver cells [17,18], such as synthesis and secretion of plasma proteins and cell surface receptors [17,19]. However, the HepG2 cell line has limited hepatocyte functionality in 2D culture [9]. Spheroids of HepG2 cells have been shown to comprise enhanced liver-like functionality compared to 2D cultures by upregulation of genes involved in liver-specific xenobiotic and lipid metabolism [4,20], and formation of bile canalicular-like structures and tight cell-cell interactions [4,21,22], making it a more realistic liver model. Compared to the 2D HepG2 cultures, HepG2 spheroids are described as cultures with a high activity of liver-specific functions, e.g. albumin [23–25], urea synthesis [23,24] and CYP expression [24–26].

3D cultures can be applied for different toxicological endpoints [3,5]. An important endpoint in hazard characterization is genotoxicity. The micronucleus assay has successfully been applied on HepG2 spheroids to detect chromosomal damage [26]. The comet assay is a very useful technique for screening of genotoxic potential of compounds. Several genotoxic endpoints can be detected, such as DNA strand breaks (SBs) and oxidized or alkylated base lesions [27–33], and the comet assay can provide an early prediction of a compound's mutagenic and carcinogenic potential [34,35]. Thus, the development of protocols for application of 3D cultures for genotoxicity assessment (via e.g. the comet assay) is needed for a better and more precise prediction of adverse effects on human health after environmental exposure.

The current study is, to our knowledge, the first study on the application of the comet assay to spheroidal HepG2 cultures. Colchicine (COL), chlorpromazine hydrochloride (CHLO), and methyl methanesulfonate (MMS) were used for cytotoxicity evaluation, and MMS and hydrogen peroxide (H_2O_2) were used for evaluating potential differences in response and sensitivity of genotoxicity in 2D and 3D HepG2 cultures.

2. Materials and methods

2.1. Cultivation of HepG2 cells

HepG2 cells, provided from the ECACC-European Collection of Authenticated Cell Cultures (cell line no. 85011430, Salisbury, United Kingdom) and Leibniz-Institut DSMZ-Deutsche Sammlung von Mikroorganismen und Zellkulturen GmbH (cell line no. ACC-180, Braunschweig, Germany), were cultured in Dulbecco's modified Eagle's medium (DMEM D6046 with low glucose and 4 mM L-glutamine, Sigma-Aldrich) or Roswell Park Memorial Institute medium (RPMI 1640, R8758, Sigma-Aldrich) supplemented with 10% v/v fetal bovine serum (FBS, 26140-079 ThermoFisher Scientific), 100 U/ml penicillin and 100 µg/ml streptomycin (5070-63, ThermoFisher Scientific). Experiments were performed in two independent laboratories. For experiments at NILU (Laboratory 1) with cells from ECACC DMEM was used, and RPMI was used at Fraunhofer IBMT (Laboratory 2) for cells from DSMZ. Cells were passaged two times a week using phosphate buffered saline (PBS, 14190094, ThermoFisher) for washing and dry trypsinization with trypsin-EDTA 0.25% (59429C, Sigma-Aldrich) or wet trypsinization with trypsin-EDTA 0.05% (25-052-CI, Corning).

2.2. Preparation of 3D spheroid cultures

Drops (20 µl) of HepG2 cells were pipetted to the inside of a lid of a petri dish (312, 625, 1250, 2500, 5000 cells per 20 µl; 65 drops per dish), and carefully placed on top of the dish filled with 5 ml cell culture medium. After 4 days incubation at 37 °C 5% CO_2, the spheroids (one spheroid formed per drop) were transferred by pipetting to a 96-well spheroid culture plate (Corning). One spheroid was placed per well. The spheroids were further incubated for additional 21 days for size and circularity measurements, with medium renewal (4/5 vol) every two days. For all exposure studies, conditions with 2500 cells per drop, 4 days in hanging drop and one week in low adhesion plate were selected. Day 1 of the presented results is the day after transfer of the spheroids to plates. For trypsinization, the spheroids were washed twice with PBS, incubated with 50 µl 0.25% trypsin-EDTA for 10 min and neutralized in 150 µl fresh medium. The whole content of the well was transferred to an Eppendorf tube and centrifuged for 5 min at 200 *g*. The supernatant was removed, and the pellet re-suspended, before 30 µl medium was added for samples for cell counting and 70 µl medium was added for samples used for the comet assay.

2.3. Preparation of 2D cultures

Parallel to experiments with spheroids, standard *in vitro* 2D cultures were used. HepG2 cells were seeded at 20,000 cells/well in a standard flat 96-well plate for the comet assay and alamarBlue assay, 10,000 cells/well for measuring metabolic capacity of cells, and 200,000 cells/well in flat 24-well plate for flow cytometry analysis. The 2D cultures were then incubated overnight prior to exposure to test substances or fresh medium. For trypsinization, 2D cultures were washed twice with PBS, dry trypsinized for 4 min and re-suspended in cell culture medium.

2.4. Cell counting

The cells were counted in automated cell counter Countess® (C10227, Invitrogen). The cell suspension was mixed 1:1 with trypan-blue (0.4%, Invitrogen) for staining of cells with compromised cell membrane.

2.5. Evaluation of metabolic status of 2D and 3D cultures

The levels of albumin, alanine transaminase (ALT), aspartate aminotransferase (AST) and glutamate dehydrogenase (GDH) in 2D and 3D cultures were measured after 8 days in culture. Albumin was measured with kit BCG Albumin Assay Kit (Cell Biolabs, USA), ALT with Alanine Aminotransferase (ALT or SGPT) Activity Colori-metric/Fluorometric Assay Kit (Biovision, USA), AST with Aspartate Aminotransferase (AST) Activity Colorimetric Assay Kit (Biovision), and GDH with Glutamate Dehydrogenase (GDH) Activity Colorimetric Assay Kit (Biovision). All assays were performed according to the manufacturers' protocols. For the albumin assay, FBS-free medium was used. Values were normalized to the number of cells per 2D or 3D culture on day of measurement.

2.6. Size measurements of the spheroids

For measuring the size (diameter and area) of the spheroids, images were acquired in the bright field microscope Leica DM-IL microscope with camera (Moticam) and the software Motic Images (Laboratory 1), and Olympus IX70 microscope with CC-12 camera (Olympus) and the software i-cell (Laboratory 2). The images of 8–18 spheroids per experiment were analyzed with the software Fiji Is Just ImageJ (Fiji) [36] using the same settings for all images. Also the circularity of the spheroids was analyzed via Fiji.

2.7. Fluorescence imaging of the spheroids

The spheroids were stained with fluorescein diacetate (FDA, Invitrogen) and propidium iodide (PI, Invitrogen) to allow for visualization of live and dead cells, respectively. The spheroids were incubated in dark at room temperature with 30 µg/ml FDA and 40 µg/ml PI for up to 10 min, before washing with PBS and imaging in PBS in confocal microscope Zeiss LSM 700 with the software ZEN2010 (Zeiss). At least three spheroids were imaged per sample in two independent experiments (n = 2).

2.8. Test substances and exposure

HepG2 cells in 2D and 3D culture were exposed in 96-well plates to COL, CHLO or MMS (1–750 µM) for 24 h, using at least two (2D) or three (3D) parallel wells per experiment, each with one culture or spheroid. As negative control complete chemical-free culture medium was used, with at least four (2D) or five (3D) parallel wells per experiment. For both 2D and 3D cultures the same volumes and concentrations were used. Stock solutions of COL (cat.no. A13240.03, VWR International), MMS (cat. no. 129925, Sigma-Aldrich), and CHLO (cat. no. C8138, Sigma-Aldrich) were freshly prepared before all experiments. COL was dissolved in sterile PBS (10 mM), MMS was dissolved in dimethyl sulfoxide (DMSO) and sterile PBS at a ratio of 1:1.8:9 (1 M) before dilution in PBS (10 mM), and CHLO was dissolved in sterile filtered ultrapure water (5 mM). Working solutions were prepared by serial dilution in cell culture medium.

HepG2 cells in 2D and 3D cultures were exposed also to H_2O_2 (7722841, Sigma-Aldrich). 2D and 3D cultures were exposed both as cells in culture in 96-well plates and as disintegrated single cells, to 12.5–250 µM H_2O_2 in PBS for 5 min on ice. See Section 2.11 for further details.

2.9. Viability measured by alamarBlue assay

Spheroids or cells in 2D culture were washed twice with PBS, and alamarBlue diluted in cell culture medium (10% v/v) was added (100 µl/well for 3D, 200 µl/well for 2D). Samples were incubated at 37 °C, 5% CO_2 in dark for 3–4 h before the supernatant was transferred to a new 96-well plate (40 µl/well). Fluorescence (excitation 530 nm, emission 590 nm) was determined on a FLUOstar OPTIMA microplate reader. Per exposure well, four 2D samples and two 3D samples were measured in parallel, and at least two 2D or three 3D exposure wells were used per experiment. Blank values (alamarBlue without cells present) were subtracted from the measured fluorescence intensity, which was further normalized by the average measurement of the unexposed samples, giving the relative viability of the exposed samples.

2.10. Viability measured by flow cytometry

The exposure medium was removed and the cells were washed with PBS. Cells of the 2D model were detached with trypsin and transferred into tubes. Cells of two parallel culture wells treated with the same conditions were transferred into the same tube. In case of the 3D model, three spheroids treated with the same conditions were transferred in one tube and trypsinized. Cells were centrifuged at 200 *g* for 3 min and washed again with PBS. Cells were stained with 30 µg/ml FDA solution for 1 min. After an additional washing step with PBS the cells were fixed in fixing solution (1% paraformaldehyde, 0.85% NaCl in PBS, pH 7.4) and analyzed with a FACS Calibur (BD Biosciences, USA) at 488 nm. Viability measurement by flow cytometry were performed with internal duplicates (2D) or triplicates (3D).

2.11. DNA damage measured by the comet assay

The miniaturized 12-gel comet assay was performed as described by El Yamani et al. (2017) [37]. Briefly, exposed 2D and 3D cultures were disaggregated with trypsin as described above, and re-suspended in 150 µl and 70 µl fresh medium, respectively. For embedding of cells in gels, 50 µl cell suspension was mixed 1:3 with low melting point-agarose (0.8% w/v, A9414, Sigma-Aldrich, 37 °C) in a 96-well plate, giving a final agarose concentration of 0.6% w/v. Mini-gels (10 µl) were made on microscope slides pre-coated with 0.5% standard melting point agarose (05066, Sigma-Aldrich), and submerged in lysis solution (2.5 M NaCl, 0.1 M EDTA, 10 mM Tris, 10% v/v Triton X-100, pH 10, 4 °C) for at least 1 h.

In addition to the alkylating agent MMS, H_2O_2 was used as a positive control for DNA SBs. 2D and 3D cultures were exposed both as cells in culture and as disintegrated single cells. For cells in culture, the 2D and 3D cultures were exposed to 12.5–250 µM H_2O_2 for 5 min on ice, washed in PBS, trypsinized and embedded in gels as described above. For exposure of single cells from 2D and 3D cultures, control, non-treated cells were embedded into gels on slides and the gels were submerged in 12.5–100 µM H_2O_2 in PBS for 5 min at 4 °C, washed twice for 5 min in PBS (4 °C) and then submerged in a separate coplin jar of lysis solution.

For detection of oxidized or alkylated bases, the modified comet assay was used with the bacterial repair enzyme formamidopyrimidine DNA glycosylase (Fpg, gift from Professor Andrew Collins, University of Oslo, Norway), which converts oxidized or alkylated bases to SBs [33]. After lysis, slides with cells embedded in gels were washed twice for 8 min in buffer F (40 mM HEPES, 0.1 M KCl, 0.5 mM EDTA, 0.2 mg/ml BSA, pH 8, 4 °C), added Fpg enzyme diluted in buffer F, and covered with a polyethylene foil and incubated at 37 °C for 30 min in a humid box. As positive control for function of Fpg enzyme, HepG2 cells were exposed to a photosensitizer Ro 19–8022 (2 µM, kindly provided by Hoffmann La Roche, Switzerland) and irradiated with visible light (30 cm distance from cells, 250 W) on ice for 4 min, before embedding into gels. The photosensitizer Ro 19-8022 with light induces oxidized purines, mainly 8-oxoG, which is detected by the Fpg enzyme [38,33].

For electrophoresis, the slides were placed in the tank, submerged in electrophoresis solution (0.3 M NaOH, 1 mM EDTA, pH > 13, 4 °C), to let the DNA unwind for 20 min, before running electrophoresis for 20 min (25 V, 1.25 V/cm, Consort EV202). The gels were neutralized in PBS, washed in ultrapure H_2O and left to dry overnight. Comets were visualized after staining with SYBR gold (1:2000, S11494, Sigma-Aldrich), and scored in Leica DMI 6000 B (Leica Microsystems), equipped with a SYBR®photographic filter (Thermo Fischer Scientific) using the software Comet assay IV 4.3.1 (Perceptive Instruments, Bury St Edmunds, UK). Median DNA tail intensity was calculated from approximately 50 comets per spheroid/sample as a measure of DNA SBs. For 3D cultures, medians were averaged from six parallel control spheroids and three parallel exposed spheroids per experiment. For 2D culture, medians were averaged from 4 parallel control samples and 2 parallel exposed samples per experiment.

2.12. Statistical analysis

Results are presented as mean with standard error of the mean (SEM) of 3 independent experiments (n = 3), unless otherwise mentioned. Effects were compared to non-treated cells, and statistical analysis by one-way ANOVA, multiple comparisons and post-test Dunnett performed in Prism/GraphPad 7. Two-way ANOVA was used for comparison between 2D and 3D cultures, with multiple comparisons and post-test Sidak. P-values are marked by * as $p < 0.05$, ** as $p < 0.01$, *** as $p < 0.001$ and **** as $p < 0.0001$. EC50 values were calculated in Prism using linear regression.

3. Results

3.1. Formation, growth and metabolic status of HepG2 spheroids

To find optimal conditions for spheroid formation via hanging drop technique and growth, different cell numbers per droplet (312–5000 cells per droplet) were studied. Spheroids were formed with all cell numbers. Spheroid area increased time-dependently until reaching a plateau after one week culture of the spheroids in a 96-well plate (after 4 days hanging drop culture) (Fig. 1). The circularity was high and stable for the spheroids seeded with lower cell numbers, and increasing over time for spheroids with higher cell numbers (Fig. 1). Based on these results, conditions with 2500 cells per drop and 4 day hanging drop culture and one week culture of the spheroids in a 96-well plate were selected for the cyto- and genotoxicity experiments.

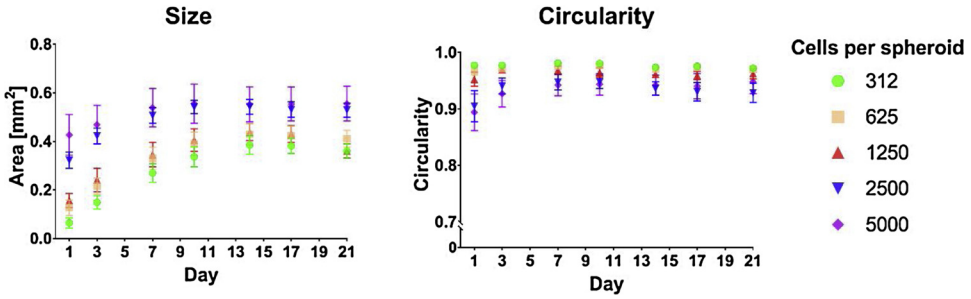

Fig. 1. Size and circularity of HepG2 spheroids. 312–5000 cells were seeded as hanging drops and cultured for 4 days before transferred to a spheroid culture plate. Size, measured as area, and circularity of the individual spheroids were measured over 21 days. Spheroid area and circularity determined by image analysis, show a time-dependent increase in spheroid size before reaching a plateau with a stable size and circularity. Mean with SEM (n = 3).

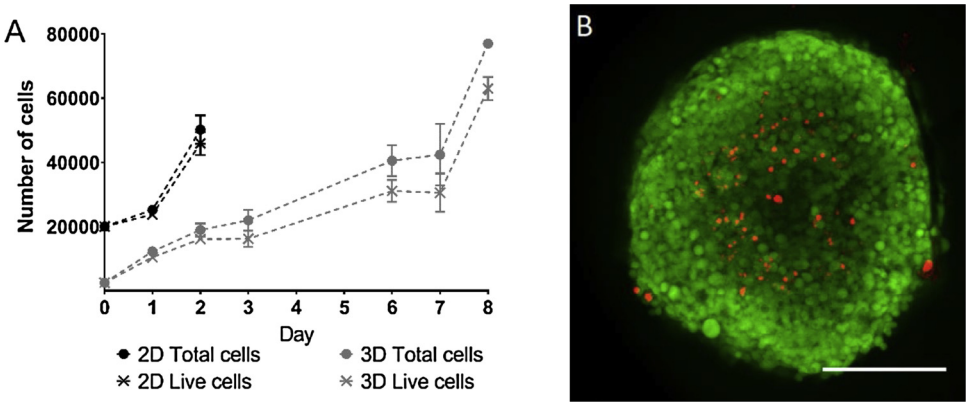

Fig. 2. Cell proliferation and viability of HepG2 cells in 2D and 3D cultures. A) The cell number in the spheroids increased over time after seeding 2500 cells, with a relatively constant viability. The number of cells in 2D cultures cultured in parallel (20.000 seeded cells) is shown as comparison. Day 0: Cell number at seeding of cells. Day 1: One day after transfer to spheroid plate (3D). Mean with SEM (n = 3). B) Representative confocal image of a spheroid at day 1, showing viable cells stained with FDA in green and a necrotic core stained with PI in red. The image is a merged image of 10 images of the spheroids cross section. A shadow is removed from the image in Fiji. Scale bar 200 µm.

Growth of the spheroids over time was investigated by measuring the diameter and counting the number of cells per spheroid. The number of cells increased in consistency with enlarged spheroid size and time (Fig. 2A). Average cell viability over time was 79% ± 2% in the 3D cultures, and 92% ± 2% in the 2D cultures, determined by the trypan blue assay. The visual analysis of the HepG2 spheroids via confocal laser scanning microscopy verified the viability of the cells in the 3D culture (Fig. 2B). The distribution of live and dead cells in the spheroids was investigated by FDA/PI staining. A small necrotic core was seen, and the viability was stable over time. A representative image of the HepG2 spheroid at day 1 is shown in Fig. 2B, with a high presence of viable cells.

An inter-laboratory comparison for investigating reproducibility and reliability of the development and cultivation of HepG2 liver spheroids was performed. The spheroids were cultured in laboratory 1 and laboratory 2 using the same protocol. Spheroid diameter was determined over 8 days. The growth rate was found to differ slightly, but the spheroid diameter was found to be similar both at start of culture and at time of exposure, increasing from 630 µm to 800 µm (Fig. 3).

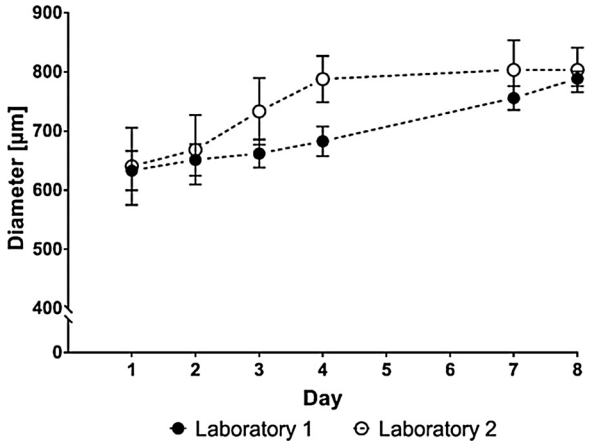

Fig. 3. Inter-laboratory comparison of HepG2 spheroid diameter. Both laboratories used the same protocol for culturing the spheroids, and achieved an increasing spheroid size, with approximately the same diameter at day 8, the end of the culture period. Day 1: One day after the transfer to spheroid plate. Mean with SEM (n = 3). No statistical differences were found between the results from the two laboratories, using two-way ANOVA with multiple comparisons and post-test Sidak.

To compare the metabolic status of the 2D and 3D HepG2 cultures, the albumin production as well as the activity of the liver-specific enzymes AST, ALT and GDH were measured (Fig. 4). Albumin concentration (2D: 7.6 µg/10^9 cells, 3D: 1.7 µg/10^9 cells) and ALT activity (2D: 27.0 units/10^9 cells, 3D: 8.5 units µg/10^9 cells), measured at day 8, was significantly increased in cultures grown as monolayers compared to spheroidal HepG2 cultures. In contrast GDH (2D: 3.4 units/10^9 cells, 3D: 9.3 units/10^9 cells) was significantly increased in the spheroidal HepG2 cultures. No significant difference was seen comparing the AST activity in 2D and 3D HepG2 cultures (Fig. 4).

3.2. Cytotoxicity studies in 2D and 3D HepG2 cultures

To investigate and compare toxicological responses of 2D and 3D HepG2 cultures, the monolayer and the spheroidal culture were exposed to COL, CHLO or MMS. Cytotoxicity was determined both by alamarBlue assay which measures metabolic activity and by flow cytometry which measures cell vitality/membrane damage (Fig. 5). Cell viability of HepG2 2D cultures, measured by alamarBlue assay, was reduced by exposure to COL. Already at 10 µM, COL induced a significant decrease in relative cell viability, whereas in 3D liver cultures an exposure with the highest tested concentration (750 µM) did not result in a significant decrease in relative cell viability (Fig. 5A). Statistically significant differences were found between 2D and 3D cultures for 5 and 10 µM COL where the relative cell viability of 3D cultures were high. By flow cytometry, no effect of COL was seen in either 2D or 3D cultures (Fig. 5D). In contrast, CHLO induced in both models (2D and 3D) a concentration dependent decrease in relative cell viability, but with different sensitivity (Fig. 5B). EC50 values were calculated for CHLO in 2D culture to be 93 µM (alamarBlue assay) and 177 µM (flow cytometry analysis), respectively. For 3D cultures the EC50 values were

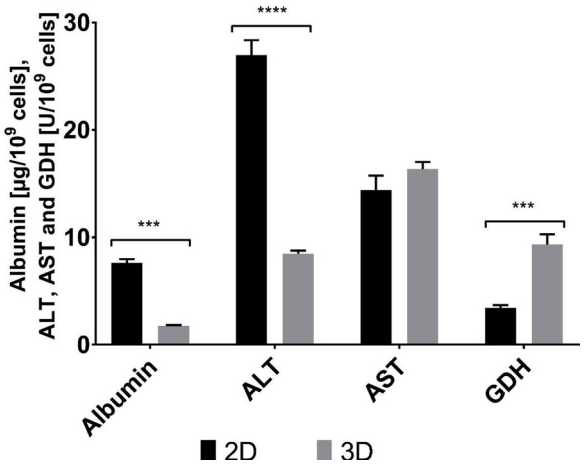

Fig. 4. Metabolic status of 2D and 3D HepG2 cultures at day 8. Amounts of released albumin, AST, ALT and GDH from HepG2 cells are dependent on culture conditions. Numbers are normalized to number of live cells per culture at time of measurement. Similar results would be seen if presented as mass or unit per volume. Mean with SEM (n = 3). Two-way ANOVA with multiple comparisons and post-test Sidak was performed to compare 2D and 3D results. *** $p < 0.001$; **** $p < 0.0001$.

higher; 227 µM measured by alamarBlue assay and > 750 µM by flow cytometry (Fig. 5B and 5E, Table 1). MMS was cytotoxic at the highest tested concentrations in 2D culture, with an EC50 value of 417 µM by alamarBlue assay (Fig. 5C, Table 1). No significant reduction in relative cell viability was observed at the highest concentration for 3D culture (Fig. 5F, Table 1).

Confocal imaging of exposed spheroids showed an increase in the amount of dead cells by PI staining after exposure to 750 µM MMS and 300 µM CHLO, but no effect after COL exposure (Fig. 6). The staining was successful for cells mainly at the surface of the spheroid (Fig. A.1 and A.2). In summary, all three compounds induced cytotoxicity to HepG2 cells in 2D cultures, measured by alamarBlue assay (Fig. 5A–C). Only CHLO and MMS were cytotoxic for 3D cultures, determined by alamarBlue assay (Fig. 5E) and confocal imaging (Fig. 6).

3.3. Genotoxicity measured in 2D and 3D cultures by the comet assay

The background level of damage in non-treated 3D cultures was 5.1% ± 1.3% DNA in tail for DNA SBs and 8.7% ± 1.6% for DNA SBs plus Fpg sites. Corresponding values for 2D cultures were 4.8% ± 0.6% and 5.1% ± 1.4%. The background levels for 2D and 3D cultures are in the same range. The control for function of Fpg (Ro 19-8022) was within the expected range, as the Fpg treated control had an increase of at least 20% DNA in tail compared to the control without Fpg (data not shown). For genotoxicity studies by the comet assay only MMS and H_2O_2 were selected because they are direct acting mutagens and the most common positive controls in the comet assay. When exposing 2D and 3D cultures to H_2O_2 in the culture wells, before trypsinization, the induction of SBs in 2D cultures was significant at a concentration of 50 µM and above (Fig. 7A). A smaller increase in SBs was seen for 3D cultures treated with H_2O_2 as spheroids before trypsinization. When exposing disaggregated single cells after trypsinization, both 2D and 3D cultured cells had high levels of DNA SBs at all tested concentrations (Fig. 7B).

HepG2 monolayer and spheroids were treated with MMS for 24 h before disaggregation of cells and DNA damage investigation. A concentration related response was seen after the MMS exposure, both for DNA SBs and DNA SBs + Fpg (Fig. 8). In 3D cultures, significantly increased DNA damage relative to control was found already at 50 µM MMS. The responses of 2D and 3D cultures were significantly different from each other at 100 µM and 300 µM, where a higher induced damage was seen in 3D cultures.

4. Discussion

In this study a liver spheroid model was established and the suitability for genotoxicity studies by the comet assay was investigated. HepG2 2D cultures are commonly used for evaluating toxicity of chemicals, drugs and nanoparticles [9,44–46]. They are easy to handle and are frequently used for high-throughput toxicity screening, but have also disadvantages. The adherent monolayer cell culture is far removed from the *in vivo* morphology, and this could account for the altered metabolism compared to 3D tissue structure. 3D cell models, such as spheroids, represent a much more *in vivo*-like morphology and behavior and are thus a more realistic model. Ramaiahgari et al. concludes that the 3D model better is more sensitive than monolayer cultures and better predicts potential hepatotoxicity, especially when increasing the exposure time from 24 h to repeated exposures [22]. Therefore, the development of a new liver spheroid model combined with the comet assay is in-line with the 3R concept and meets the strong need for new *in vitro* models for genotoxicity screening under realistic *in vivo*-like conditions. Kermanizadeh et al. used the commercialized InSphero liver spheroids for comet assay studies [39]. Our study is, to the best of our knowledge, the first to focus on the application of the comet assay to HepG2 liver spheroids cultured in a simple and reproducible manner. The protocol used here for the spheroid preparation and cultivation has not yet been published before. Published protocols differ in cell numbers, culture conditions and durations, and droplet volumes [26].The implementation of the developed protocol in two independent laboratories, using HepG2 cells from different sources and with different cell culture media, confirmed a high reproducibility, in contrast to a study by Hurrell et al. [40]. The background levels of DNA SBs in 2D and 3D cultures were similar and within the recommended range for human cells [27,41].

The increase in number of cells during the first week of spheroid culture is consistent with other studies on HepG2 and primary hepatocytes [40,42]. The plateau of the spheroid area after about one week in culture (Fig. 1) could indicate a reduced proliferation index of the spheroidal cells [40], and/or a decreased level of the proliferation marker Ki67 [22]. The observed necrotic core in the spheroids is characteristic of cultures with diameters > 300 µm [4].

The metabolic status of HepG2 cells cultured in 2D and 3D was measured by the presence of different proteins and enzyme activity. The production of albumin is an indicator for metabolic activity [43], ALT, AST and GDH are *in vivo* liver functionality biomarkers. Upon liver injury, the serum concentrations of ALT, AST and GDH increase [43,44]. In contrast to published studies [4,22,26], the albumin production in HepG2 spheroids was lower than in 2D monolayers (Fig. 4). Shah et al. reported a higher albumin secretion in hanging spheroids on day 4 compared to day 7 [26]. One reason for the low albumin concentration could be the late time point (day 8) in our study. Additionally, the albumin secretion could depend on the spheroid size. Nishikawa et al. determined the highest albumin level in the smallest spheroids (200 µm), and albumin levels similar to ours were found in larger spheroids and monolayers [45]. One can speculate over the possibility of the cells in the spheroids being packed too tightly for the albumin to pass through to the surface, resulting in a lower albumin concentration in the supernatant where the quantification takes place. Comparing the results of the 2D and 3D HepG2 cultures, ALT decreased, AST remained relatively constant and GDH increased in the spheroidal model, suggesting a difference in the metabolic status of the cells. In the 3D spheroid culture approach, all cells are in contact with other cells but not with an artificial matrix. The spheroid approach supports much more the maintenance of *in vivo*-like cell morphology and behavior than 2D approaches.

After characterizing the HepG2 liver spheroids, the cytotoxicity in 2D and 3D cultures was evaluated to determine the concentrations for

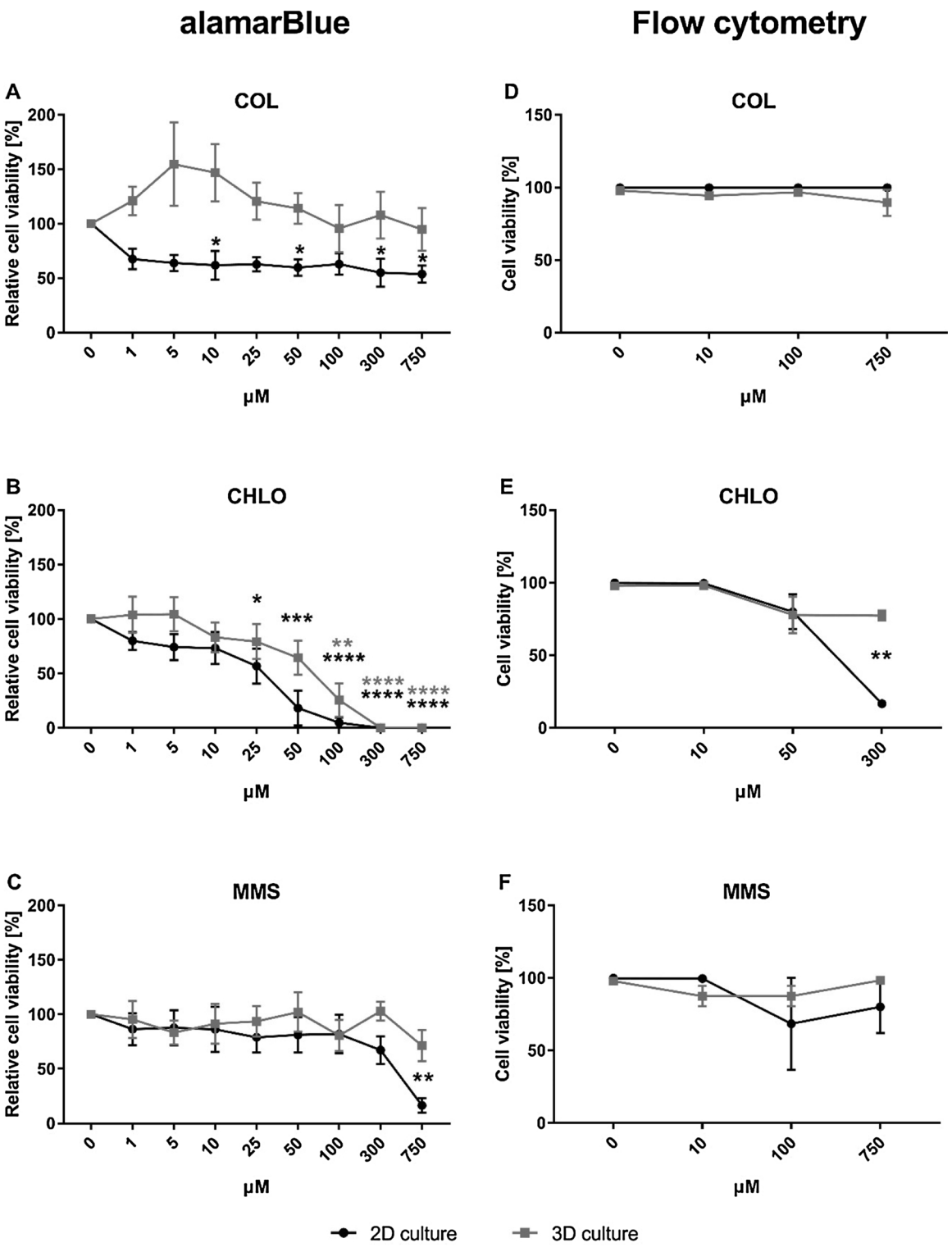

Fig. 5. Effect of COL, CHLO and MMS on cell viability of 2D and 3D HepG2 cultures, measured by alamarBlue assay (endpoint: metabolic activity) (A–C) and flow cytometry (endpoint: cell vitality/ membrane damage) (D–F) after 24 h exposure. COL reduced the relative cell viability of 2D cultures in the alamarBlue assay but no viability reduction was seen by flow cytometry analysis after FDA/PI staining. CHLO was cytotoxic for both 2D and 3D cultures. MMS was cytotoxic at high concentrations for 2D culture in alamarBlue assay. Mean with SEM and n = 3, except for 3D cultures in alamarBlue assay where n = 5. One-way ANOVA with multiple comparisons and post-test Dunnett was performed to compare effect to negative control. * $p < 0.05$; ** $p < 0.01$; *** $p < 0.001$; **** $p < 0.0001$. Statistically significant differences were seen between 2D and 3D results only for COL 5 µM and 10 µM ($p < 0.05$), using two-way ANOVA with multiple comparisons and post-test Sidak.

Table 1
EC50 values of the test compounds COL, CHLO and MMS.

	alamarBlue		Flow cytometry	
	2D	3D	2D	3D
COL	> 750 µM	> 750 µM	> 750 µM	> 750 µM
CHLO	93 µM	227 µM	177 µM	> 750 µM
MMS	417 µM	> 750 µM	> 750 µM	> 750 µM

the comet assay. Three different cytotoxicity assays (alamarBlue assay, live/dead staining with flow cytometry, confocal imaging) were applied. The alamarBlue assay showed an effect of COL, CHLO and MMS in 2D cultures, but only with CHLO on 3D cultures. Confocal imaging showed however that MMS induced cytotoxic effects in 3D cultures. The cell viability assay with flow cytometry showed a smaller effect or no effect. The differences in the effects between the methods may reflect differences in their modes of action. The alamarBlue assay measures the cells' ability to metabolize the substrate resazurin, PI stains DNA in cells that have lost their membrane integrity, whereas FDA is hydrolyzed to the fluorescent fluorescein in viable cells. The smaller or no effect on the viability measured by flow cytometry may in addition be due to the loss of dead cells during the washing steps which are not performed with the other cytotoxicity assays. This illustrates the importance of including more than one assay or endpoint to evaluate the cytotoxicity of a substance. A statistically significant difference in induced cytotoxicity when comparing 2D and 3D cultures, was seen only for low concentrations of COL evaluated by alamarBlue assay. Greater variation, however, was seen for 3D cultures than 2D cultures with alamarBlue (Fig. 5), possibly related to variations in spheroid size.

In vivo and *in vitro* studies have shown that CHLO, a tricyclic antidepressant, is intrinsically toxic to the liver as it can induce cholestasis and hepatic necrosis [46]. The concentration-related cytotoxicity after exposure to CHLO (Fig. 5, Table 1) was similar to that reported by Xuan et al. [47]. Similar EC50 values were obtained for 2D and 3D cultures in a study on HepaRG cells [11]. However, Mueller et al. used spheroids of HepG2 and HepaRG cells, and found lower CHLO EC50 values for 2D cultures compared to 3D cultures after 72 h exposure [48].

COL, a drug for treatment of acute gout, binds to tubulin and inhibits cell division [49] leading to decreased metabolism of the cell culture. Consistent with this, COL was cytotoxic in 2D cultures (Fig. 5) – but not in 3D culture, possibly owing to differences in cellular metabolism in the spheroid or poor penetration of the compound into the spheroid.

MMS is a mutagenic compound [50] that methylates DNA bases, leading to SBs, chromosome breaks, micronucleus formation, and finally cell death [51,52]. The effect of MMS on cell viability (Figs. 5, 6) was seen mainly at the highest test concentrations. MMS was, in addition, able to induce genotoxicity in HepG2 2D and 3D cultures in a concentration related manner (Fig. 8) at non-cytotoxic concentrations. There was slightly more DNA damage after MMS exposure of 3D compared to 2D cultures. A similar HepG2 spheroid model, tested with other chemicals, had a higher sensitivity to micronucleus formation [26].

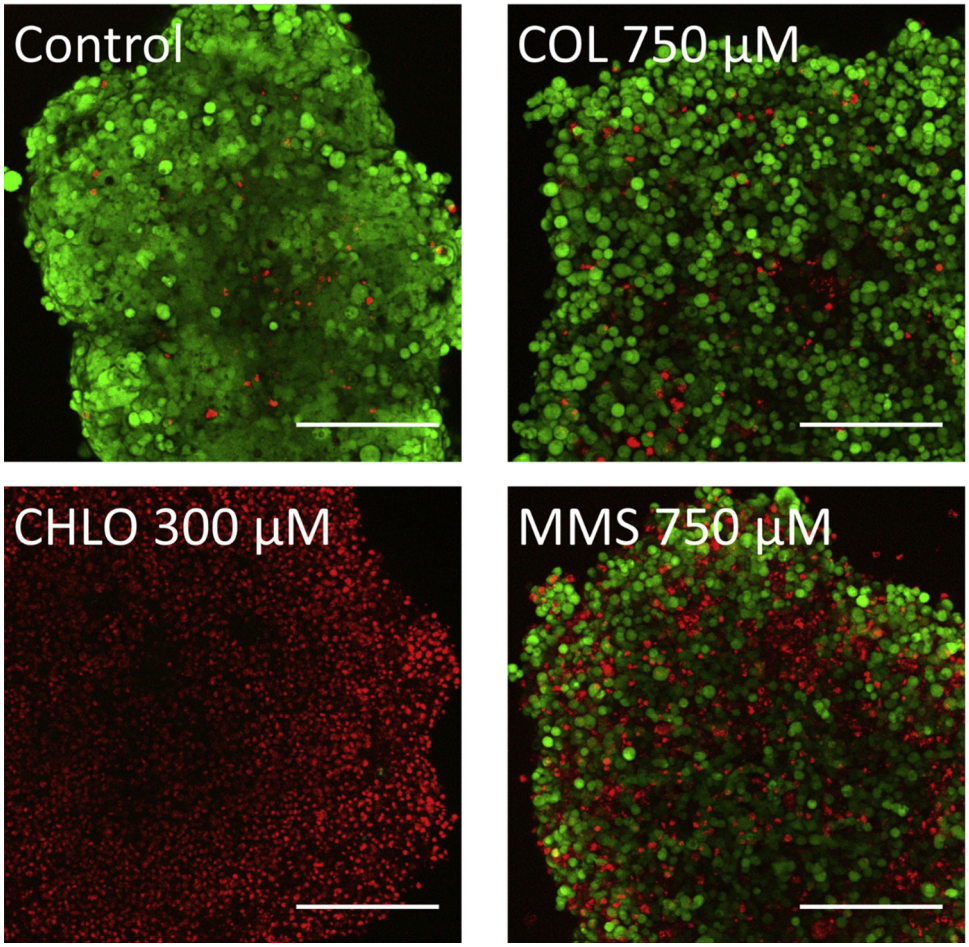

Fig. 6. Representative images from confocal microscopy of exposed HepG2 spheroids. Spheroids were exposed to COL, CHLO and MMS for 24 h before viable (green) and dead (red) cells were stained with FDA (green) and PI (red). The images are z-stack projections from the spheroid surface to approximately 150 µm towards the spheroid core. Scale bar 200 µm.

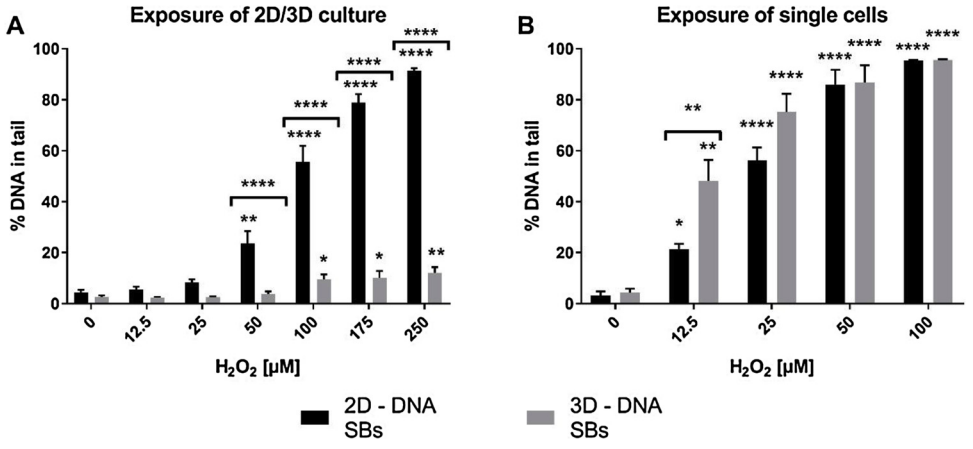

Fig. 7. DNA damage in H_2O_2 exposed HepG2 2D and 3D culture measured by the comet assay. H_2O_2 induced DNA SBs in HepG2 cells exposed either in (A) 2D or 3D culture where the cultures were treated with H_2O_2 for five minutes before disaggregation of the cells and embedding of cells in gel, and (B) as single cells where the cells were incubated with H_2O_2 for five minutes after trypsinization and embedding of cells in gel. The level of DNA SBs was higher for single cell exposure than for monolayer/spheroid exposure. Mean with SEM (n = 3). One-way ANOVA with multiple comparisons and post-test Dunnett was performed to compare effect to negative control. Two-way ANOVA with multiple comparisons and post-test Sidak was performed to compare 2D and 3D results. * $p < 0.05$; ** $p < 0.01$; *** $p < 0.001$; **** $p < 0.0001$.

H_2O_2 exposure of disaggregated cells from 3D cultures induced elevated levels of DNA SBs at lower concentrations than in cells from 2D cultures. Exposure of intact 2D and 3D cultures to non-cytotoxic concentrations of H_2O_2 [53,54] (Fig. 7A) led to fewer DNA SBs compared with exposure of disaggregated single cells in the gel (Fig. 7B). One reason for this difference could be the fast repair of SBs during disaggregation of cells after exposure [54]. 3D cultures required longer time for disaggregation of cells, compared to 2D cultures, resulting in a higher level of damage in 2D cultures. Also, it has been reported that the incubation time and concentration of trypsin and EDTA can affect the background level of SBs in HepG2 cells [55]. Additionally, it is possible that the tested compounds in this study did not fully diffuse inside the spheroid, thus accounting for differences in the observed results between 2D and 3D cultures. Concentration gradients of oxygen, proteins, waste and other solutes have been shown to be present in tissues or 3D cultures [6,9]. However, in a study by Gaskell et al. the exposure of autofluorescent doxorubicin was found to be homogenous throughout the spheroid volume in a C3A liver spheroid [56]. In contrast, limited fluorescence of dyes was found in the middle of the center of breast cancer spheroids [57]. A similar effect was observed in our study with PI and FDA at the end of the culture period, where the dyes stained mainly the outer parts of the spheroid and did not reach the center and so measuring cytotoxicity in this way may not be completely reliable.

Cell density, incubation time, pH, spheroid size, the surrounding extracellular matrix (ECM), and factors involved with bioaccumulation, such as lipophilicity, could potentially be important for the chemical's distribution in the spheroid [58]. However, heterogeneous exposure of spheroids can possibly also be closer to *in vivo* exposure, with the cellular arrangements and metabolic zonation through the acinus. The investigation of the influence of the location of the cells in the spheroid on the genomic damage could give more detailed information [59].

5. Conclusions

The present study demonstrates the successful application of the comet assay to HepG2 liver spheroids, bridging the gap between *in vivo* studies and assays based on 2D monolayers. We tested a liver spheroid model in two independent laboratories, with successful application for both genotoxicity studies via the comet assay and several cytotoxicity assays. Compared to traditional 2D monolayer culture, spheroidal cultures can have higher variability; however, due to the different geometrical arrangements of the cells, they reflect much better the *in vivo* situation. Depending on the objective of the study, it should be considered which cell model is best suited for the investigations. Time- and cost-efficient 2D models are usually sufficient for pre-screening in the field of pharmaceutical drug development. However, if effects in complex systems or the interaction of several cell responses or different cell types should be considered, 3D spheroids are more realistic models that comply with the 3Rs policy to reduce *in vivo* testing. Our study is a positive contribution to the development of advanced *in vitro* models. Future studies with HepG2 spheroids should focus on increasing the relevance towards the human liver, by including co-cultures of hepatocytes with macrophages and longer or repeated exposure.

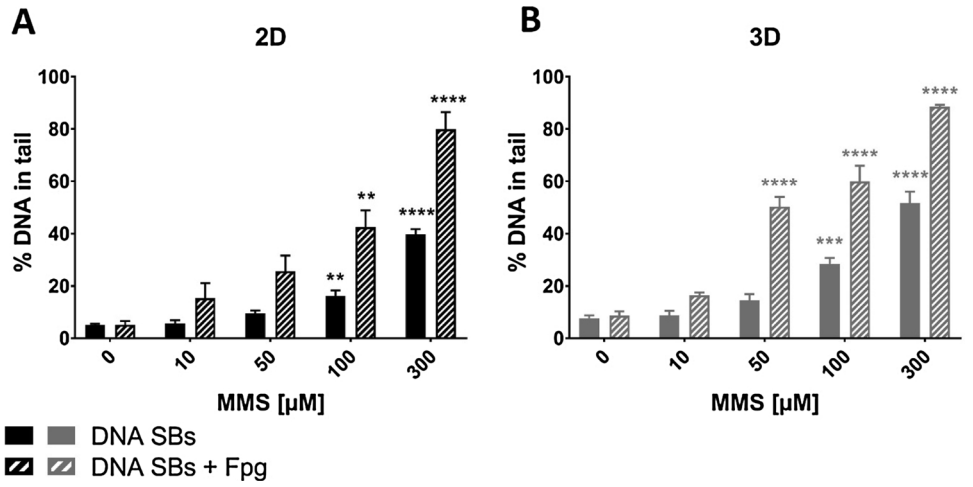

Fig. 8. DNA damage in MMS exposed HepG2 2D and 3D cultures measured by the comet assay. HepG2 monolayer (A) and spheroids (B) were treated with MMS for 24 h before disaggregation of cells and DNA damage investigation. The % DNA in tail is increasing with increasing MMS concentration, for both 2D and 3D cultures. Mean with SEM (n = 3). In 3D culture significant difference from control was found already at 50 µM MMS. 2D (A) and 3D cultures (B) were significantly different from each other ($P < 0.01$) at 100 µM and 300 µM, using two-way ANOVA with multiple comparisons and post-test Sidak. One-way ANOVA with multiple comparisons and post-test Dunnett was performed to compare effect to negative control. ** $p < 0.01$; *** $p < 0.001$; **** $p < 0.0001$.

Conflicts of interest

The authors declare that there are no conflicts of interest.

Acknowledgments

The authors would like to thank Iren E. Sturtzel for technical assistance, Hoffmann La Roche for providing the Ro 19-8022, and Andrew Collins for providing the Fpg enzyme.

Funding

This work was supported by the European Commission under the Horizon2020 program (grant agreement no 685817, HISENTS), the hCOMET project (COST Action, CA 15132), and the Norwegian Research Council (272412/F40).

Appendix A. Supplementary data

Supplementary material related to this article can be found, in the online version, at doi:https://doi.org/10.1016/j.mrgentox.2019.03.006.

References

[1] E. Commission, Regulation (EC) No. 1907/2006 of the European Parliament and the Council of 18 December 2006 Concerning the Registration, Evaluation, Authorisation and Restriction of Chemicals (REACH), Establishing a European Chemical Agency, (1999), pp. 451–849.
[2] S.S. Bale, et al., In vitro platforms for evaluating liver toxicity, Exp. Biol. Med. (Maywood) 239 (9) (2014) 1180–1191, https://doi.org/10.1177/1535370214531872.
[3] S.J. Evans, et al., Critical review of the current and future challenges associated with advanced in vitro systems towards the study of nanoparticle (secondary) genotoxicity, Mutagenesis 32 (1) (2017) 233–241, https://doi.org/10.1093/mutage/gew054.
[4] J.A. Kyffin, et al., Impact of cell types and culture methods on the functionality of in vitro liver systems - A review of cell systems for hepatotoxicity assessment, Toxicol. In Vitro 48 (2018) 262–275, https://doi.org/10.1016/j.tiv.2018.01.023.
[5] C. Calitz, et al., Recent advances in three-dimensional cell culturing to assess liver function and dysfunction: from a drug biotransformation and toxicity perspective, Toxicol. Mech. Methods 28 (5) (2018) 369–385, https://doi.org/10.1080/15376516.2017.1422580.
[6] L.G. Griffith, M.A. Swartz, Capturing complex 3D tissue physiology in vitro, Nat. Rev. Mol. Cell Biol. 7 (3) (2006) 211–224, https://doi.org/10.1038/nrm1858.
[7] S. Breslin, L. O'Driscoll, Three-dimensional cell culture: the missing link in drug discovery, Drug Discov. Today 18 (5–6) (2013) 240–249, https://doi.org/10.1016/j.drudis.2012.10.003.
[8] A. Astashkina, D.W. Grainger, Critical analysis of 3-D organoid in vitro cell culture models for high-throughput drug candidate toxicity assessments, Adv. Drug Deliv. Rev. 69-70 (2014) 1–18, https://doi.org/10.1016/j.addr.2014.02.008.
[9] P. Godoy, et al., Recent advances in 2D and 3D in vitro systems using primary hepatocytes, alternative hepatocyte sources and non-parenchymal liver cells and their use in investigating mechanisms of hepatotoxicity, cell signaling and ADME, Arch. Toxicol. 87 (8) (2013) 1315–1530, https://doi.org/10.1007/s00204-013-1078-5.
[10] A.J. Harris, S.L. Dial, D.A. Casciano, Comparison of basal gene expression profiles and effects of hepatocarcinogens on gene expression in cultured primary human hepatocytes and HepG2 cells, Mutat. Res. 549 (1-2) (2004) 79–99, https://doi.org/10.1016/j.mrfmmm.2003.11.014.
[11] Z. Wang, et al., HepaRG culture in tethered spheroids as an in vitro three-dimensional model for drug safety screening, J. Appl. Toxicol. 35 (8) (2015) 909–917, https://doi.org/10.1002/jat.3090.
[12] Z.H. Jiao, et al., Hormesis effects of silver nanoparticles at non-cytotoxic doses to human hepatoma cells, PLoS One 9 (7) (2014) e102564, https://doi.org/10.1371/journal.pone.0102564.
[13] S. Wilkening, F. Stahl, A. Bader, Comparison of primary human hepatocytes and hepatoma cell line Hepg2 with regard to their biotransformation properties, Drug Metab. Dispos. 31 (8) (2003) 1035–1042, https://doi.org/10.1124/dmd.31.8.1035.
[14] K. Nakamura, et al., Expression of albumin and cytochrome P450 enzymes in HepG2 cells cultured with a nanotechnology-based culture plate with microfabricated scaffold, J. Toxicol. Sci. 36 (5) (2011) 625–633.
[15] T. Anada, et al., An oxygen-permeable spheroid culture system for the prevention of central hypoxia and necrosis of spheroids, Biomaterials 33 (33) (2012) 8430–8441, https://doi.org/10.1016/j.biomaterials.2012.08.040.
[16] N.B. Javitt, Hep G2 cells as a resource for metabolic studies: lipoprotein, cholesterol, and bile acids, FASEB J. 4 (2) (1990) 161–168, https://doi.org/10.1096/fasebj.4.2.2153592.
[17] A. Nowrouzi, et al., Cytotoxicity of subtoxic AgNP in human hepatoma cell line (HepG2) after long-term exposure, Iran. Biomed. J. 14 (1-2) (2010) 23–32.
[18] S.C. Sahu, et al., Comparative cytotoxicity of nanosilver in human liver HepG2 and colon Caco2 cells in culture, J. Appl. Toxicol. 34 (11) (2014) 1155–1166, https://doi.org/10.1002/jat.2994.
[19] F. Faedmaleki, et al., Toxicity effect of silver nanoparticles on mice liver primary cell culture and HepG2 cell line, Iran. J. Pharm. Res. 13 (1) (2014) 235–242.
[20] T.T. Chang, M. Hughes-Fulford, Monolayer and spheroid culture of human liver hepatocellular carcinoma cell line cells demonstrate distinct global gene expression patterns and functional phenotypes, Tissue Eng. Part A 15 (3) (2009) 559–567, https://doi.org/10.1089/ten.tea.2007.0434.
[21] J.M. Kelm, et al., Method for generation of homogeneous multicellular tumor spheroids applicable to a wide variety of cell types, Biotechnol. Bioeng. 83 (2) (2003) 173–180, https://doi.org/10.1002/bit.10655.
[22] S.C. Ramaiahgari, et al., A 3D in vitro model of differentiated HepG2 cell spheroids with improved liver-like properties for repeated dose high-throughput toxicity studies, Arch. Toxicol. 88 (5) (2014) 1083–1095, https://doi.org/10.1007/s00204-014-1215-9.
[23] M. Bokhari, et al., Culture of HepG2 liver cells on three dimensional polystyrene scaffolds enhances cell structure and function during toxicological challenge, J. Anat. 211 (4) (2007) 567–576, https://doi.org/10.1111/j.1469-7580.2007.00778.x.
[24] L. Meli, et al., Influence of a three-dimensional, microarray environment on human cell culture in drug screening systems, Biomaterials 33 (35) (2012) 9087–9096, https://doi.org/10.1016/j.biomaterials.2012.08.065.
[25] Y. Miki, et al., The advantages of co-culture over mono cell culture in simulating in vivo environment, J. Steroid Biochem. Mol. Biol. 131 (3-5) (2012) 68–75, https://doi.org/10.1016/j.jsbmb.2011.12.004.
[26] U.K. Shah, et al., A three-dimensional in vitro HepG2 cells liver spheroid model for genotoxicity studies, Mutat. Res. 825 (2018) 51–58, https://doi.org/10.1016/j.mrgentox.2017.12.005.
[27] M. Dusinska, A.R. Collins, The comet assay in human biomonitoring: gene-environment interactions, Mutagenesis 23 (3) (2008) 191–205, https://doi.org/10.1093/mutage/gen007.
[28] A.R. Collins, et al., High throughput toxicity screening and intracellular detection of nanomaterials, Wiley Interdiscip. Rev. Nanomed. Nanobiotechnol. 9 (1) (2017), https://doi.org/10.1002/wnan.1413.
[29] M. Dusinska, A. Collins, Detection of oxidised purines and UV-induced photoproducts in DNA, by inclusion of lesion-specific enzymes in the comet assay (single cell gel electrophoresis), Alta- Altern. Lab. Anim. 24 (1996) 405–411.
[30] S. Boiteux, et al., Homogeneous Escherichia coli FPG protein. A DNA glycosylase which excises imidazole ring-opened purines and nicks DNA at apurinic/apyrimidinic sites, J. Biol. Chem. 265 (7) (1990) 3916–3922.
[31] S. Boiteux, et al., Substrate specificity of the Escherichia coli Fpg protein (formamidopyrimidine-DNA glycosylase): excision of purine lesions in DNA produced by ionizing radiation or photosensitization, Biochemistry 31 (1) (1992) 106–110.
[32] G. Speit, et al., Sensitivity of the FPG protein towards alkylation damage in the comet assay, Toxicol. Lett. 146 (2) (2004) 151–158.
[33] A.R. Collins, The use of bacterial repair endonucleases in the comet assay, in: J.-C. Gautier (Ed.), Drug Safety Evaluation: Methods and Protocols, Springer New York, New York, NY, 2017, pp. 173–184.
[34] S.H. Kang, et al., Recent advances in in vivo genotoxicity testing: prediction of carcinogenic potential using comet and micronucleus assay in animal models, J. Cancer Prev. 18 (4) (2013) 277–288.
[35] Y.H. Hong, et al., Assessment of the predictive capacity of the optimized in vitro comet assay using HepG2 cells, Mutat. Res. 827 (2018) 59–67, https://doi.org/10.1016/j.mrgentox.2018.01.010.
[36] J. Schindelin, et al., Fiji: an open-source platform for biological-image analysis, Nat. Methods 9 (7) (2012) 676–682, https://doi.org/10.1038/nmeth.2019.
[37] N. El Yamani, et al., In vitro genotoxicity testing of four reference metal nanomaterials, titanium dioxide, zinc oxide, cerium oxide and silver: towards reliable hazard assessment, Mutagenesis 32 (1) (2017) 117–126, https://doi.org/10.1093/mutage/gew060.
[38] A. Azqueta, et al., Comet assay to measure DNA repair: approach and applications, Front. Genet. 5 (2014) 288, https://doi.org/10.3389/fgene.2014.00288.
[39] A. Kermanizadeh, et al., Hepatic toxicology following single and multiple exposure of engineered nanomaterials utilising a novel primary human 3D liver microtissue model, Part. Fibre Toxicol. 11 (1) (2014) 56, https://doi.org/10.1186/s12989-014-0056-2.
[40] T. Hurrell, et al., Characterization and reproducibility of HepG2 hanging drop spheroids toxicology in vitro, Toxicol. In Vitro 50 (2018) 86–94, https://doi.org/10.1016/j.tiv.2018.02.013.
[41] P. Moller, The alkaline comet assay: towards validation in biomonitoring of DNA damaging exposures, Basic Clin. Pharmacol. Toxicol. 98 (4) (2006) 336–345, https://doi.org/10.1111/j.1742-7843.2006.pto_167.x.
[42] C.C. Bell, et al., Characterization of primary human hepatocyte spheroids as a model system for drug-induced liver injury, liver function and disease, Sci. Rep. 6 (2016) 25187, https://doi.org/10.1038/srep25187.
[43] X. Yang, et al., Chapter 13: hepatic toxicity biomarkers, in: R. Gupta (Ed.), Biomarkers in Toxicology, Elsevier, USA, 2014.
[44] J. Ozer, et al., The current state of serum biomarkers of hepatotoxicity, Toxicology 245 (3) (2008) 194–205, https://doi.org/10.1016/j.tox.2007.11.021.
[45] T. Nishikawa, et al., Optimization of albumin secretion and metabolic activity of cytochrome P450 1A1 of human hepatoblastoma HepG2 cells in multicellular spheroids by controlling spheroid size, Biol. Pharm. Bull. 40 (3) (2017) 334–338, https://doi.org/10.1248/bpb.b16-00833.

[46] J.P. Buchweitz, et al., Underlying endotoxemia augments toxic responses to chlorpromazine: is there a relationship to drug idiosyncrasy? J. Pharmacol. Exp. Ther. 300 (2) (2002) 460–467.
[47] J. Xuan, et al., Development of HepG2-derived cells expressing cytochrome P450s for assessing metabolism-associated drug-induced liver toxicity, Chem. Biol. Interact. 255 (2016) 63–73, https://doi.org/10.1016/j.cbi.2015.10.009.
[48] D. Mueller, et al., 3D organotypic HepaRG cultures as in vitro model for acute and repeated dose toxicity studies, Toxicol. In Vitro 28 (1) (2014) 104–112, https://doi.org/10.1016/j.tiv.2013.06.024.
[49] Y. Finkelstein, et al., Colchicine poisoning: the dark side of an ancient drug, Clin. Toxicol. (Phila) 48 (5) (2010) 407–414, https://doi.org/10.3109/15563650.2010.495348.
[50] World Health Organization, I.A.f.R.o.C.I, IARC Monographs on the Evaluation of Carcinogenic Risks to Humans, (1999).
[51] M.D. Wyatt, D.L. Pittman, Methylating agents and DNA repair responses: Methylated bases and sources of strand breaks, Chem. Res. Toxicol. 19 (12) (2006) 1580–1594, https://doi.org/10.1021/tx060164e.
[52] M.Y. Lee, et al., Alkylating agent methyl methanesulfonate (MMS) induces a wave of global protein hyperacetylation: implications in cancer cell death, Biochem. Biophys. Res. Commun. 360 (2) (2007) 483–489, https://doi.org/10.1016/j.bbrc.2007.06.084.
[53] D. Slamenova, et al., Carboxymethyl chitin-glucan (CM-CG) protects human HepG2 and HeLa cells against oxidative DNA lesions and stimulates DNA repair of lesions induced by alkylating agents, Toxicol. In Vitro 24 (7) (2010) 1986–1992, https://doi.org/10.1016/j.tiv.2010.08.015.
[54] M. Dusinska, A. Collins, Detection of oxidised purines and UV-induced photo-products in DNA, by inclusion of lesion-specific enzymes in the comet assay (single cell gel electrophoresis), Atla- Altern. Lab. Anim. 24 (1996) 405–411.
[55] M. Uhl, C. Helma, S. Knasmuller, Single-cell gel electrophoresis assays with human-derived hepatoma (Hep G2) cells, Mutat. Res. 441 (2) (1999) 215–224.
[56] H. Gaskell, et al., Characterization of a functional C3A liver spheroid model, Toxicol. Res. (Camb) 5 (4) (2016) 1053–1065, https://doi.org/10.1039/c6tx00101g.
[57] S. Lemmo, et al., Optimization of Aqueous biphasic tumor spheroid micro-technology for anti-cancer drug testing in 3D culture, Cell. Mol. Bioeng. 7 (3) (2014) 344–354, https://doi.org/10.1007/s12195-014-0349-4.
[58] D.J. Kerr, et al., The effect of adriamycin and 4'-deoxydoxorubicin on cell survival of human lung tumour cells grown in monolayer and as spheroids, Br. J. Cancer 54 (3) (1986) 423–429.
[59] A. Nagelkerke, P.N. Span, Staining against phospho-H2AX (gamma-H2AX) as a marker for DNA damage and genomic instability in cancer tissues and cells, Adv. Exp. Med. Biol. 899 (2016) 1–10, https://doi.org/10.1007/978-3-319-26666-4_1.